Supporting Information

Synergistic Effect of Sandwich Polyoxometalates and Copper-Imidazole Complexes for Enhancing Peroxidase-like Activity

Dong-Feng Chai,‡[b] Zhuo Ma,‡[d] Hong Yan,[b] Yun-Feng Qiu,*[a,e] Hong Liu,*[b] Hua-Dong Guo,[c] and Guang-Gang Gao*[b,c]

[a] State Key Laboratory of Urban Water Resource and Environment, Harbin Institute of Technology, Harbin 150090, China. E-mail: qiuyf@hit.edu.cn (Y. Qiu)

[b] Department of Chemistry, College of Pharmacy, Jiamusi University, Jiamusi 154004, China. E-mail: hliu@jmsu.edu.cn (H. Liu), gaogg@jmsu.edu.cn (G. Gao)

[c] Department of Chemistry, Changchun Normal University, Changchun 130032, China.

[d] School of Life Science and Technology, Harbin Institute of Technology, 92 West Dazhi Street, Harbin, Heilongjiang, 150001, China.

[e] Key Laboratory of Microsystems and Micronanostructures Manufacturing (Ministry of Education), Harbin Institute of Technology, Harbin 150080, China.

‡ These authors made equal contributions to this work.

Contents:

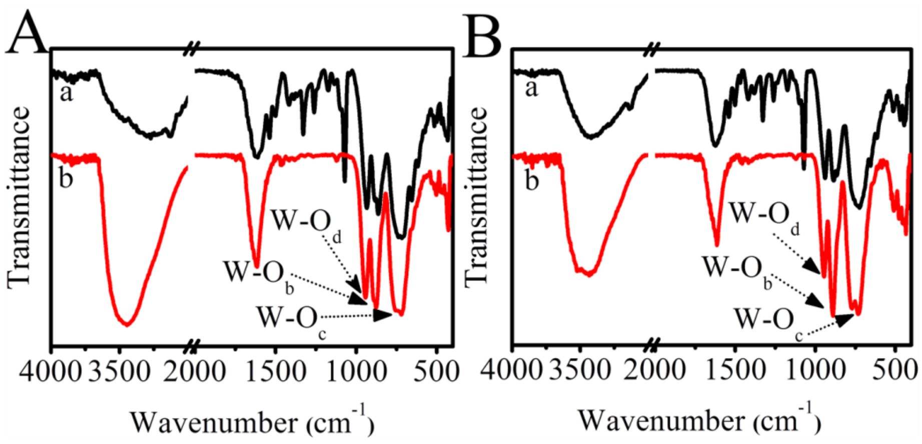

Fig. S1 (A) FTIR spectra of **1** (a, black curve) and BiW_9Cu_3 precursor (b, red curve); (B) FTIR spectra of **2** (a, black curve) and SbW_9Cu_3 precursor (b, red curve).

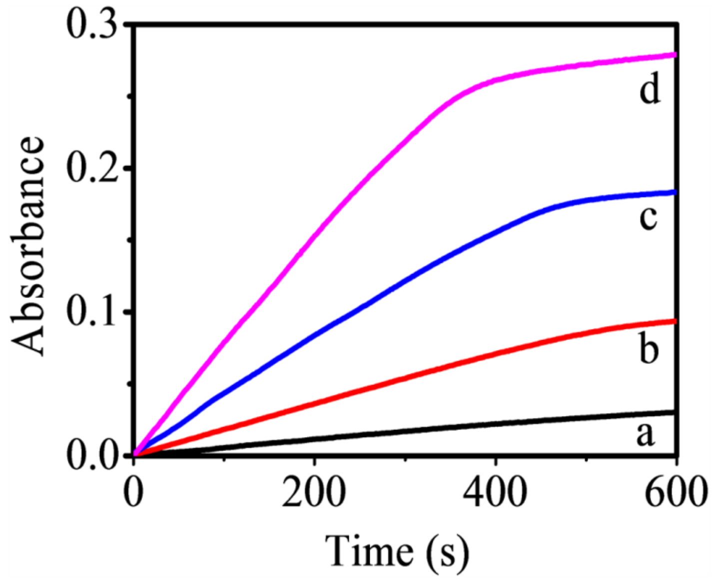

Fig. S2 Dependence of the peroxidase-like activity on the concentrations of **1** (a: 0.35×10^{-2} mg/mL, b: 0.69×10^{-2} mg/mL, c: 1.38×10^{-2} mg/ml, and d: 2.76×10^{-2} mg/mL). Experiments were conducted in time course mode in acetate buffer solution (pH = 5.5) at 55 °C.

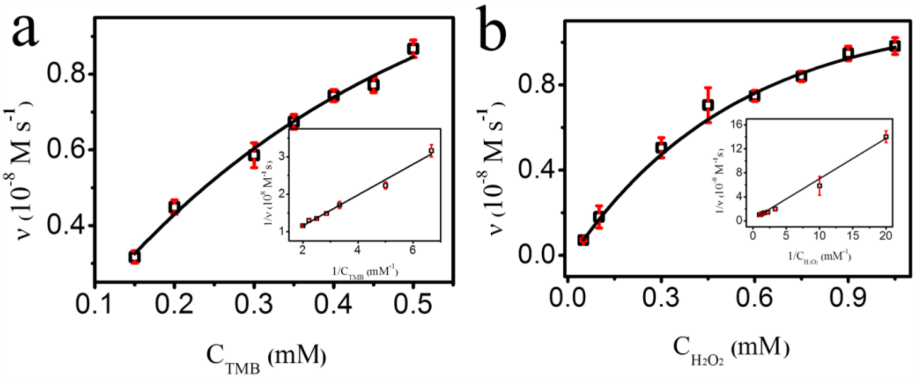

Fig. S3 Steady-state kinetic assays of **2**. (a) H_2O_2 concentration was kept constant at 100 μM and TMB concentration was varied. (b) TMB concentration was maintained at 50 μM and H_2O_2 concentration was varied. The reaction was performed in 0.1 M, pH = 5.5 acetate buffer solution at 55 °C. Details were described in the experimental section.

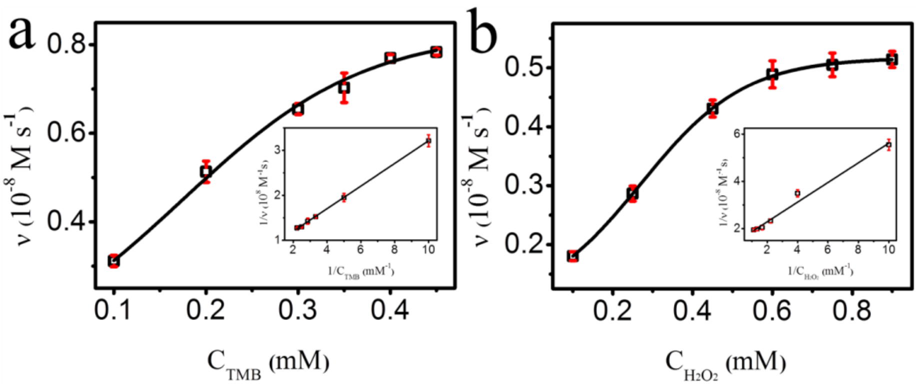

Fig. S4 Steady-state kinetic assays of BiW_9Cu_3. (a) H_2O_2 concentration was kept constant at 100 μM and TMB concentration was varied. (b) TMB concentration was maintained at 50 μM and H_2O_2 concentration was varied. The reaction was performed in 0.1 M, pH = 5.5 acetate buffer solution at 55 °C. Details were described in the experimental section.

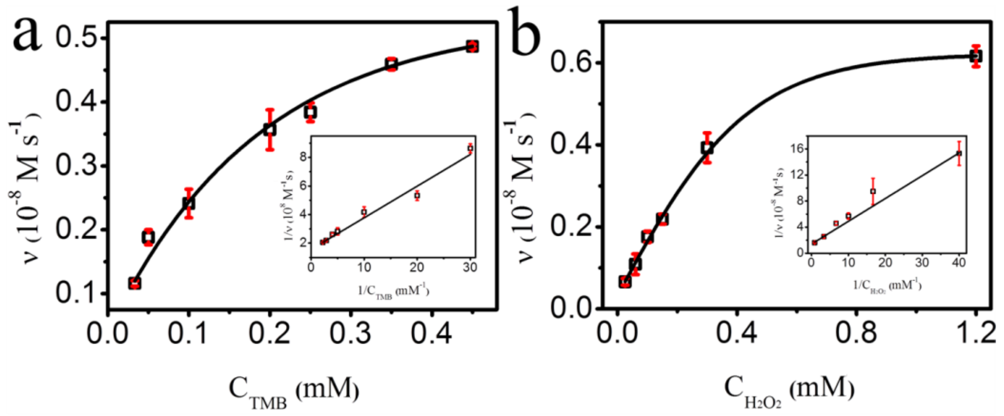

Fig. S5 Steady-state kinetic assays of SbW_9Cu_3. (a) H_2O_2 concentration was kept constant at 100 µM and TMB concentration was varied. (b) TMB concentration was maintained at 50 µM and H_2O_2 concentration was varied. The reaction was performed in 0.1 M, pH = 5.5 acetate buffer solution at 55 °C. Details were described in the experimental section.

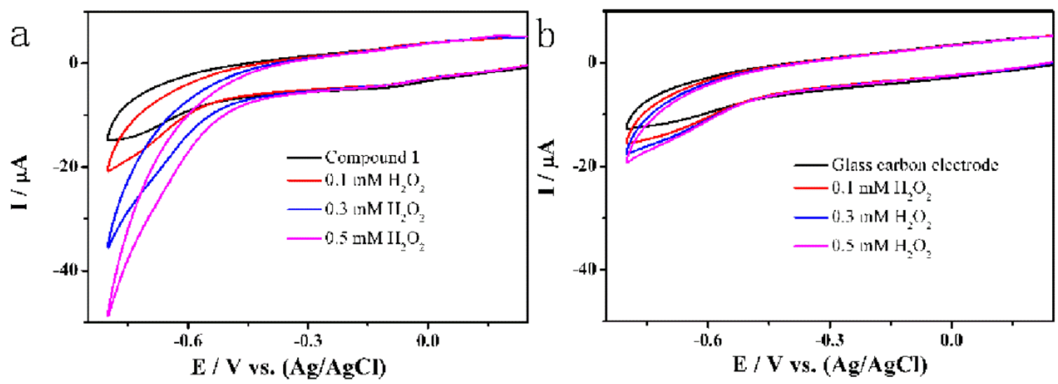

Fig. S6 CV curves of glass carbon electrode modified with (a) and without (b) compound **1** in the presence of 0.1, 0.3, and 0.5 mM H_2O_2.

We have performed the cyclic voltametry (CV) experiment of compound **1** as representative. Compound **1** was anchored on the glass carbon (GC) electrode surface by small amount of Nafion solution (5 wt%, Sigma Aldrich) for enhancing CV stability. As shown in **Fig. S6**, the reversible peak of Cu(II)/Cu(I) was not observed on bare GC, and also silent on GC with compound **1**. However, comparing with the weak signals of electro-catalytic reduction of H_2O_2 on bare GC, the signals on GC modified with compound **1** became larger. This might be related to the electro-catalytic reduction ability of compound **1**, and also high affinity between H_2O_2 and compound **1**. Further, as reported in previous work, polyoxometalates will facilitate the electro transfer from sensing targets to electron collector. Thus, this effect will also contribute to the enhancement of reducing signals of H_2O_2 on GC with compound **1**.

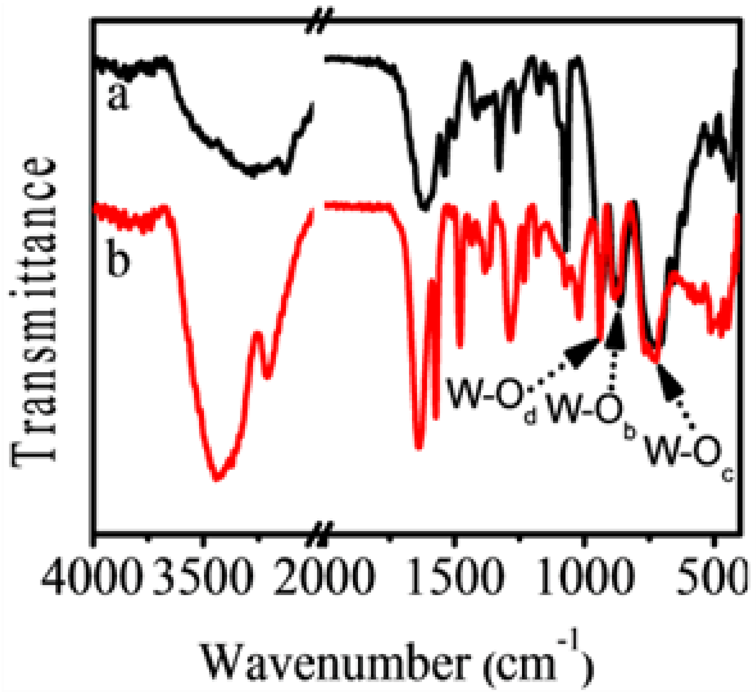

Fig. S7 FTIR spectra of **1** before (a) and after (b) reaction.

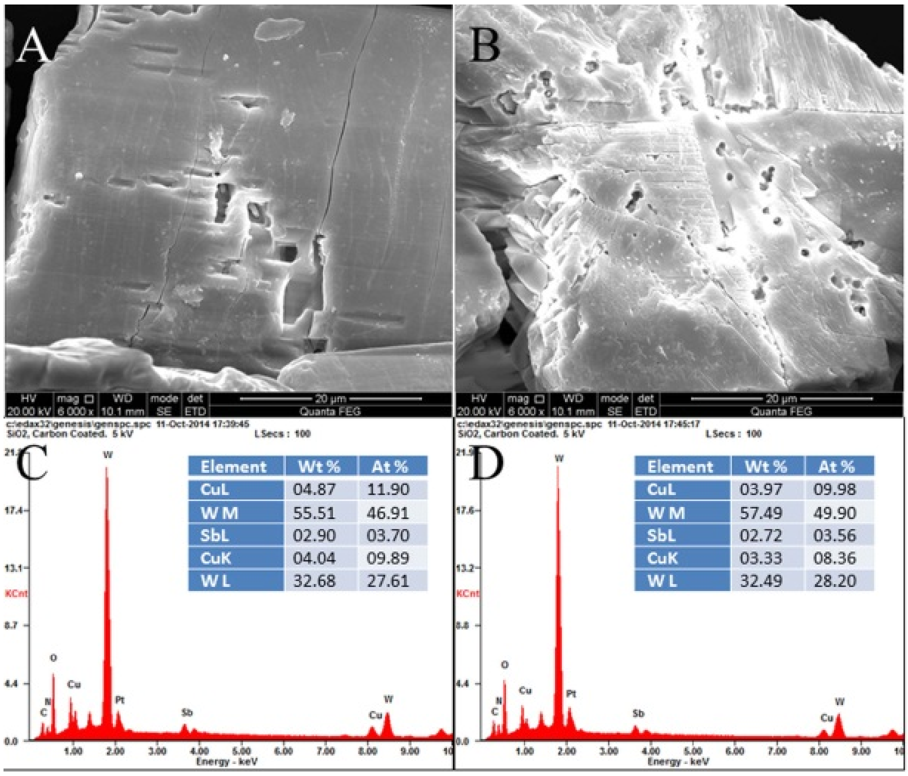

Fig. S8 (A) and (B) SEM images of ground compound **2** before and after reaction; (C) and (D) EDX before and after reaction. EDX are measured for three times to check out the consistency.

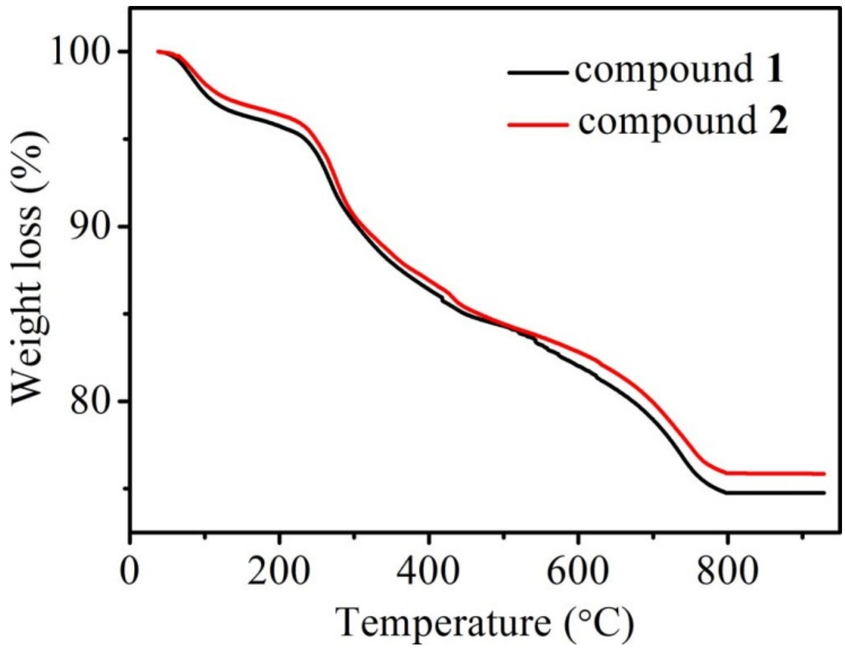

Fig. S9 TG curves for **1** and **2**.

TG analyses were performed on a NETZSCH TG 209F3 instrument under N_2 atmosphere with a heating rate of 10 K min^{-1}. The TG curve of **1** exhibits a two-step continuous weight loss process: the weight loss of 4.91% (calcd 5.00%) from 37 to 235 °C corresponds to the loss of *ca*. 19 lattice water molecules. The weight loss of 17.19% (calcd 17.08%) from 235 to 715 °C corresponds to coordinated water molecules and the decomposition of organic ligands. The TG curve of **2** exhibits a two-step continuous weight loss process: the weight loss of 4.31% (calcd 4.36%) from 37 to 235 °C corresponds to the loss of *ca*. 16 lattice water molecules. The weight loss of 17.59% (calcd 17.68%) from 235 to 730 °C corresponds to coordinated water molecules and the decomposition of organic ligands.

Table S1 Selected bond lengths (Å) and angles (°) for compound **1**.

Compound **1**					
Bi-O(32)	2.107(10)	W(6)-O(17)	2.006(12)	Cu(1)-O(19)	1.955(11)
Bi-O(31)	2.134(10)	W(6)-O(15)	2.010(11)	Cu(1)-O(34)	2.29(2)
Bi-O(33)	2.135(10)	W(6)-O(33)	2.234(10)	Cu(3)-O(22)#1	1.952(11)
W(3)-O(7)	1.694(10)	W(9)-O(29)	1.669(12)	Cu(3)-O(22)	1.952(11)
W(3)-O(21)	1.796(11)	W(9)-O(17)	1.887(11)	Cu(3)-O(23)#1	1.967(12)
W(3)-O(6)	1.957(11)	W(9)-O(30)	1.902(11)	Cu(3)-O(23)	1.967(12)
W(3)-O(9)	1.972(10)	W(9)-O(28)	1.943(10)	Cu(3)-O(40)	2.33(2)
W(3)-O(8)	2.002(11)	W(9)-O(14)	1.967(10)	C(1)-N(1)	1.36(2)
W(3)-O(32)	2.233(10)	W(9)-O(33)	2.317(10)	C(1)-C(2)	1.37(3)
W(6)-O(16)	1.702(11)	Cu(1)-O(24)	1.946(11)	C(2)-N(2)	1.33(2)
W(6)-O(24)	1.813(11)	Cu(1)-O(24)#1	1.946(11)	C(3)-N(1)	1.31(2)
W(6)-O(18)	1.918(11)	Cu(1)-O(19)#1	1.955(11)	C(3)-N(2)	1.35(2)

O(32)-Bi-O(31)	86.4(4)	O(28)-W(9)-O(33)	85.8(4)
O(32)-Bi-O(33)	87.7(4)	O(14)-W(9)-O(33)	72.5(4)
O(31)-Bi-O(33)	86.6(4)	O(24)-Cu(1)-O(24)#1	90.5(7)
O(1)-W(1)-O(19)	104.7(6)	O(24)-Cu(1)-O(19)#1	164.4(5)
O(1)-W(1)-O(3)	97.4(5)	O(24)#1-Cu(1)-O(19)#1	86.0(5)
O(19)-W(1)-O(3)	92.4(5)	O(24)-Cu(1)-O(19)	86.0(5)
O(1)-W(1)-O(18)	101.4(5)	O(24)#1-Cu(1)-O(19)	164.4(5)
O(19)-W(1)-O(18)	87.0(5)	O(19)#1-Cu(1)-O(19)	93.2(7)
O(3)-W(1)-O(18)	160.7(5)	O(24)-Cu(1)-O(34)	99.1(5)
O(1)-W(1)-O(2)	97.1(5)	O(24)#1-Cu(1)-O(34)	99.1(5)
O(19)-W(1)-O(2)	158.0(5)	O(19)#1-Cu(1)-O(34)	96.4(5)
O(3)-W(1)-O(2)	87.8(4)	O(19)-Cu(1)-O(34)	96.4(5)

Symmetry transformations used to generate equivalent atoms: #1 x, -y+3/2, z

Table S2 Selected bond lengths (Å) and angles (°) for compound **2**.

Compound **2**					
Sb-O(33)	1.991(7)	W(6)-O(18)	1.946(7)	Cu(1)-O(19)	1.954(8)
Sb-O(31)	1.996(7)	W(6)-O(17)	2.009(8)	Cu(1)-O(36)	2.359(13)
Sb-O(32)	1.997(7)	W(6)-O(31)	2.258(7)	Cu(4)-N(3)	1.951(12)
W(3)-O(7)	1.727(9)	W(9)-O(30)	1.705(8)	Cu(4)-N(1)	1.959(11)
W(3)-O(21)	1.804(8)	W(9)-O(27)	1.886(8)	Cu(4)-N(7)	1.965(11)
W(3)-O(9)	1.907(8)	W(9)-O(14)	1.908(7)	Cu(4)-N(5)	1.992(11)
W(3)-O(8)	1.989(8)	W(9)-O(26)	1.909(7)	Cu(5)-N(8)	1.952(11)
W(3)-O(6)	1.992(8)	W(9)-O(11)	1.921(8)	Cu(5)-N(11)	1.954(15)
W(3)-O(32)	2.281(7)	W(9)-O(33)	2.316(7)	Cu(5)-N(9)	1.972(11)
W(6)-O(16)	1.729(7)	Cu(1)-O(20)#1	1.946(8)	Cu(5)-N(13)	2.020(11)
W(6)-O(24)	1.794(7)	Cu(1)-O(20)	1.946(8)	Cu(5)-O(30)	2.421(8)
W(6)-O(15)	1.942(7)	Cu(1)-O(19)#1	1.954(8)	C(1)-N(2)	1.33(3)

O(33)-Sb-O(31)	90.5(3)	O(26)-W(9)-O(33)	86.3(3)
O(33)-Sb-O(32)	90.4(3)	O(11)-W(9)-O(33)	73.5(3)
O(31)-Sb-O(32)	91.7(3)	O(20)#1-Cu(1)-O(20)	88.7(5)
O(1)-W(1)-O(19)	103.8(4)	O(20)#1-Cu(1)-O(19)#1	89.4(3)
O(1)-W(1)-O(3)	102.7(4)	O(20)-Cu(1)-O(19)#1	168.1(3)
O(19)-W(1)-O(3)	90.3(3)	O(20)#1-Cu(1)-O(19)	168.1(3)
O(1)-W(1)-O(18)	97.3(3)	O(20)-Cu(1)-O(19)	89.4(3)
O(19)-W(1)-O(18)	91.4(3)	O(19)#1-Cu(1)-O(19)	90.1(5)
O(3)-W(1)-O(18)	158.9(3)	O(20)#1-Cu(1)-O(36)	98.3(4)
O(1)-W(1)-O(2)	97.5(3)	O(20)-Cu(1)-O(36)	98.3(4)
O(19)-W(1)-O(2)	158.7(3)	O(19)#1-Cu(1)-O(36)	93.6(3)
O(3)-W(1)-O(2)	86.5(3)	O(19)-Cu(1)-O(36)	93.6(3)

Symmetry transformations used to generate equivalent atoms: #1 x, -y+3/2, z